

ANALYSIS OF THE SPRINGBACK PHENOMENON USING FINITE ELEMENT METHOD

Tan Trung Le Tran^{1,2}, Thien Tich Truong^{1,2,*}

¹*Department of Engineering Mechanics, Faculty of Applied Science, Ho Chi Minh City University of Technology (HCMUT), 268 Ly Thuong Kiet Street, District 10, Ho Chi Minh City, Vietnam*

²*Vietnam National University Ho Chi Minh City, Linh Trung Ward, Thu Duc City, Ho Chi Minh City, Vietnam*

*E-mail: ttruong@hcmut.edu.vn

Received: 23 January 2024 / Revised: xx xx 2024 / Accepted: xx xx 2024

Published online: xx xx 2024

Abstract. The springback phenomenon is a significant concern in manufacturing processes, particularly in metal component forming, as it directly affects dimensional control and the shape of formed parts. Accurate prediction and analysis of springback are crucial for achieving precise dimensional control and ensuring the desired final shape. Therefore, this study focuses on analyzing the springback phenomenon using finite element method. The primary objective is to develop a Matlab program for analyzing three-dimensional springback problems. Throughout the research process, the understanding of the phenomenon has been enhanced. The developed program has been successfully implemented to model and simulate the forming process, considering various aspects of the problem. The results of the solutions have been compared and evaluated, leading to important conclusions. The research also outlines future developments in this field. It is hoped that the results and understanding of this research will contribute to the field of computational mechanics and inspire further research.

Keywords: springback, finite element method, material nonlinearity, return-mapping, elasto-plastic.

1. INTRODUCTION

Analyzing springback is crucial in manufacturing and engineering. It presents challenges to achieving dimensional accuracy and quality in fabricated components. Manufacturers can adjust tooling design, process parameters, and material selection to

minimize springback effects. Additionally, springback analysis enables optimization of manufacturing processes, leading to improved efficiency, reduced lead times, and enhanced competitiveness.

The elastic recovery of materials significantly affects the shape and dimensional accuracy of drawpieces. While springback cannot be completely eliminated, there are methods to minimize it. One approach is designing the die to account for springback. Adjusting bending process parameters can also help reduce springback. Another method involves overbending the material during die shaping [1]. The finite element method (FEM) is commonly used to predict the final shape of drawpieces [2]. FEM simulates sheet metal forming processes, providing insights into stress and deformation distribution, forming forces, and potential defects.

To reflect the nonlinear strain and stress during elastic-plastic deformation of the sheet material, the crucial point in the computational modelling of springback is the proper choice of finite element formulation, the element size and a number of integration points through the sheet thickness. Suitable mesh density, especially in the region of contact of the tools with the sheet is a balance between computational time and springback prediction accuracy. Different studies have proposed varying numbers of integration points, ranging from 5 to 51. For nonlinear analysis, five integration points yield accurate results [3], while Xu et al. [4] concluded that usually seven integration points are sufficient. However, Wagoner and Li found that up to 51 points are necessary for shell type elements to analyze springback with a 1% computational error [5]. Consequently, the choice of integration points remains an open issue in springback simulation, as noted by Banabic [6].

To gain a better understanding of the springback phenomenon, this study focuses on investigating the influence of material properties on springback. Different materials exhibit varying levels of elastic recovery, which affects the magnitude and extent of springback. By examining the stress-strain behavior, elastic modulus, yield strength, and other material properties.

This study has achieved its objectives by exploring nonlinear sources, the method for solving nonlinear systems. The development of a program to analyze the springback phenomenon in a three-dimensional problem has been successfully accomplished, and the results have been compared and evaluated. The conclusions derived from this research provide a direction for further development in the research.

2. METHODOLOGY

2.1. Newton–Raphson method

For solving nonlinear equations, the Newton–Raphson method is briefly introduced here. With the assumption of an initial estimation \mathbf{u}_0 , then adding an increment $\Delta \mathbf{u}$, so that the new estimate $\mathbf{u}_0 + \Delta \mathbf{u}$ is close to the solution of $P(u) = f$. In order to find the increment, the nonlinear equations are locally approximated by linear ones. This process is repeated until the original nonlinear equations are satisfied.

Suppose an approximate solution at the i -th iteration is known and is designated by \mathbf{u}_i . The solution at the next iteration can be approximated as follows [7]

$$\mathbf{P}(\mathbf{u}^{i+1}) \approx \mathbf{P}(\mathbf{u}^i) + \mathbf{K}_T^i(\mathbf{u}^i) \Delta \mathbf{u}^i = \mathbf{f}, \quad (1)$$

where $\mathbf{K}_T^i(\mathbf{u}^i)$ is the Jacobian matrix at the i -th iteration, $\Delta \mathbf{u}^i$ is the solution increment. Rearrange the terms, the system of linearized equations can be obtained as

$$\mathbf{K}_T^i(\mathbf{u}^i) \Delta \mathbf{u}^i = \mathbf{f} - \mathbf{P}(\mathbf{u}^i). \quad (2)$$

After solving for the displacement increment $\Delta \mathbf{u}^i$, a new approximate solution is obtained as follows

$$\mathbf{u}^{i+1} = \mathbf{u}^i + \Delta \mathbf{u}^i. \quad (3)$$

In general, this solution does not satisfy the system of nonlinear equations exactly and there are residuals defined as follows

$$\mathbf{R}^{i+1} = \mathbf{f} - \mathbf{P}(\mathbf{u}^{i+1}). \quad (4)$$

If the residual is smaller than a user-defined tolerance, the solution \mathbf{u}^{i+1} can be accepted as the solution, and the solving process stops. Otherwise, the process is repeated until this convergence criteria is met.

2.2. Return-mapping algorithm

The stress and plastic variables are determined using the return-mapping algorithm. The algorithm is briefly demonstrated through the following steps:

Step 1. Compute the trial stress ${}^{tr}\boldsymbol{\sigma} = {}^n\boldsymbol{\sigma} + \mathbf{D} \cdot \Delta \boldsymbol{\varepsilon}$.

Step 2. Compute the deviatoric stress ${}^{tr}\mathbf{s} = {}^{tr}\boldsymbol{\sigma} - \frac{1}{3} \text{tr}({}^{tr}\boldsymbol{\sigma}) \mathbf{1}$.

Step 3. Compute norm $\|{}^{tr}\mathbf{s}\| = \sqrt{({}^{tr}s_{11})^2 + ({}^{tr}s_{22})^2 + ({}^{tr}s_{33})^2 + 2[({}^{tr}s_{12})^2 + ({}^{tr}s_{23})^2 + ({}^{tr}s_{13})^2]}$.

Step 4. Define the yield function $f = \|\text{tr} \mathbf{s}\| - \sqrt{\frac{2}{3}} [\sigma_Y^0 + H e_p]$.

Step 5. Check for the yield status

IF $f < 0$: Compute the material properties

$${}^{n+1}\boldsymbol{\sigma} = {}^{tr}\boldsymbol{\sigma},$$

$$\mathbf{D}^{alg} = \mathbf{D} = \begin{bmatrix} \lambda + 2\mu & \lambda & \lambda & 0 & 0 & 0 \\ \lambda & \lambda + 2\mu & \lambda & 0 & 0 & 0 \\ \lambda & \lambda & \lambda + 2\mu & 0 & 0 & 0 \\ 0 & 0 & 0 & \mu & 0 & 0 \\ 0 & 0 & 0 & 0 & \mu & 0 \\ 0 & 0 & 0 & 0 & 0 & \mu \end{bmatrix}.$$

END IF

Step 6. Define the consistency parameter $\gamma = \frac{f}{2\mu + \frac{2}{3}H}$ and the unit deviatoric

vector $\mathbf{N} = \frac{{}^{tr}\mathbf{s}}{\|\text{tr} \mathbf{s}\|}$.

Step 7. Update stress ${}^{n+1}\boldsymbol{\sigma} = {}^{tr}\boldsymbol{\sigma} - 2\mu\gamma\mathbf{N}$.

Step 8. Update effective plastic strain ${}^{n+1}e_p = {}^n e_p + \sqrt{(2/3)\gamma}$.

Step 9. Compute the consistent tangent stiffness $D_{ij}^{alg} = D_{ij} - (c_1 - c_2) N_i N_j - c_2 \times I_{ij}^{dev}$, where

$$c_1 = \frac{4\mu^2}{2\mu + \frac{2}{3}H}, \quad c_2 = \frac{4\mu^2\gamma}{\|\text{tr} \mathbf{s}\|},$$

$$\mathbf{I}^{dev} = \begin{bmatrix} 2/3 & -1/3 & -1/3 & 0 & 0 & 0 \\ -1/3 & 2/3 & -1/3 & 0 & 0 & 0 \\ -1/3 & -1/3 & 2/3 & 0 & 0 & 0 \\ 0 & 0 & 0 & 1/2 & 0 & 0 \\ 0 & 0 & 0 & 0 & 1/2 & 0 \\ 0 & 0 & 0 & 0 & 0 & 1/2 \end{bmatrix}.$$

3. NUMERICAL RESULTS AND DISCUSSIONS

3.1. Partially loaded elasto-plastic block

The first example is a 3-dimensional elasto-plastic block under partial compression as shown in Fig. 1(a). The load's magnitude for this example is $p = 800$ MPa. Due to the symmetry of the problem, only one-quarter of the block as depicted in Fig. 1(b) is

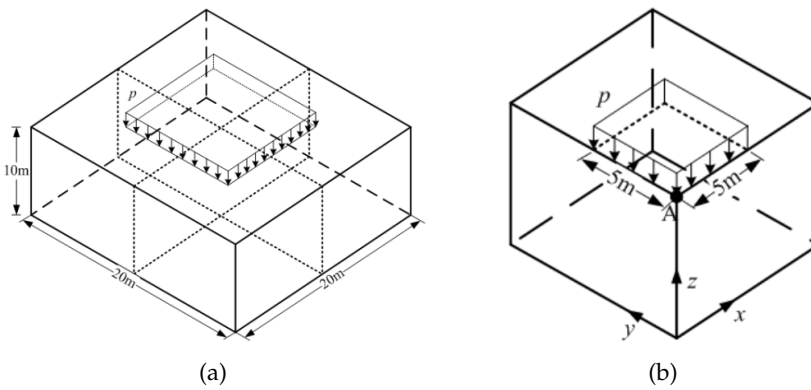


Fig. 1. (a) The full model of a block under partial compression, and (b) The quarter model

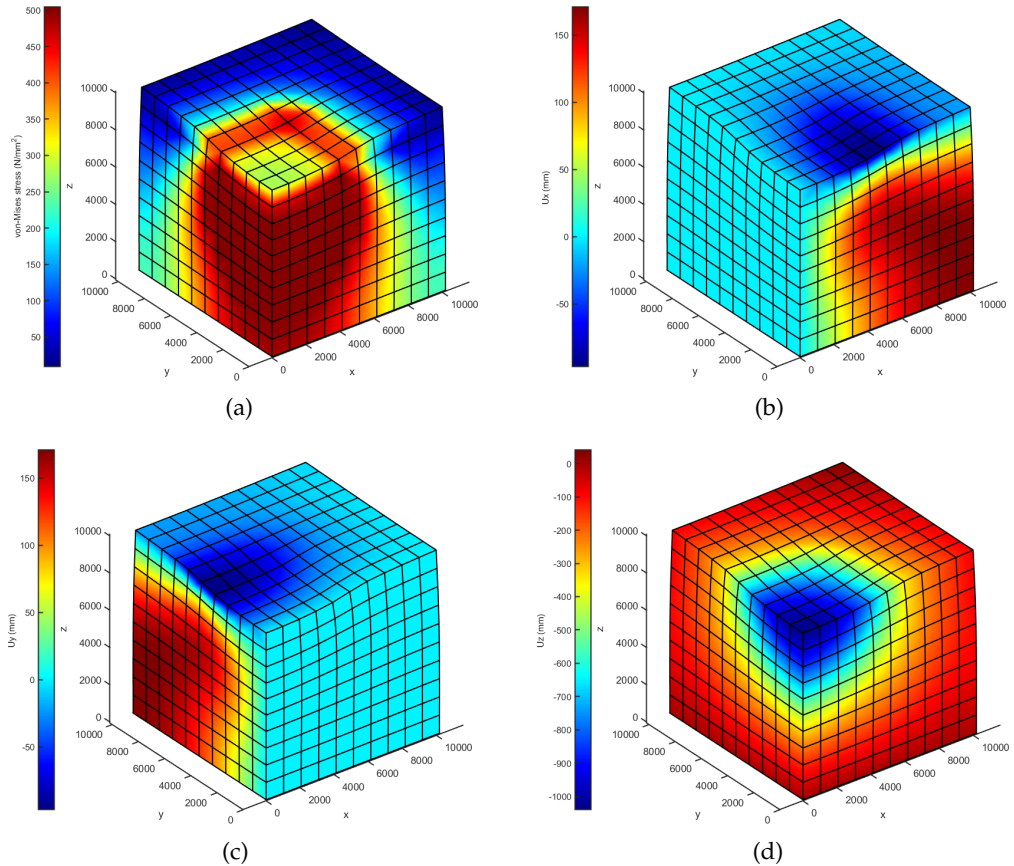


Fig. 2. (a) The von Mises stress (unit: MPa), (b) The displacement u_x (unit: mm), (c) The displacement u_y (unit: mm), (d) The displacement u_z (unit: mm)

sufficient to be modeled to save the computational time. The material model is assumed to be perfect elasto-plastic model and the material properties are given as Young’s modulus $E = 6900$ MPa, Poisson’s ratio $\nu = 0.3$, tangent modulus $E_t = 0$ MPa, yield strength $\sigma_y = 500$ MPa. The model is represented by FEM’s discretization with 1310 nodes and 1000 hexahedron elements.

Upon comparing the results obtained from the finite element Matlab program (present study) with those presented in the reference [8] (as shown in Table 1), it is evident that the relative error is small. This observation highlights the reliability of the elasto-plastic analysis program for 3D problems, as it generates reliable results. The distributions of the displacement field and the von Mises stress of the quarter of the block are shown in Fig. 2.

Table 1. The von Mises stress and displacement components of the block

Quantity	Present study	Reference [8]	Error (%)
u_x (m)	0.17	0.18	1.25
u_y (m)	0.17	0.18	1.25
u_z (m)	1.13	1.10	2.73
von Mises stress (MPa)	518	500	2.80

3.2. Axial torsion behavior of the square column

This example analyses the springback phenomenon of a square column subjected to torsional loading with two loading processes: loading and unloading. The dimensions of the square column are $A = 20$ mm, $B = 20$ mm, $C = 200$ mm as shown in Fig. 3(a). The square column, due to its solid model and being subjected to torsional forces on all four

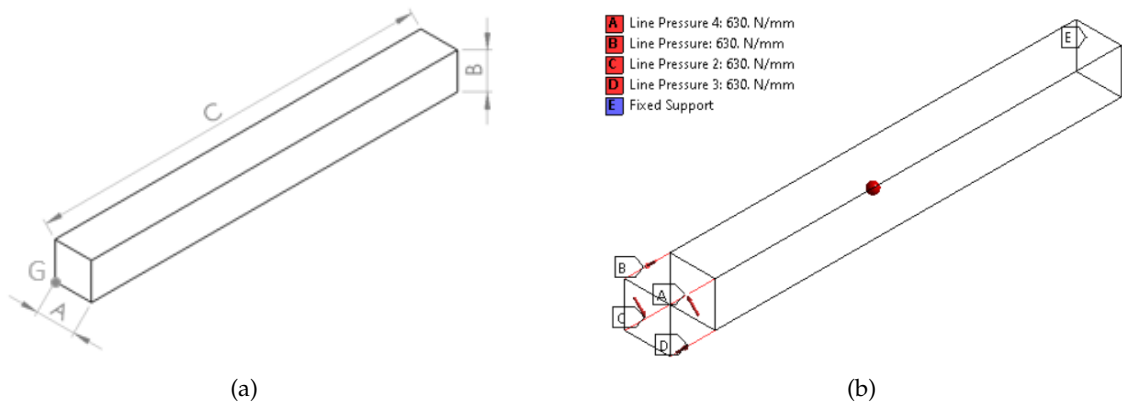


Fig. 3. (a) The square column, and (b) The model with boundary conditions

sides (see Fig. 3(b)). The material model is bilinear and the material properties are given as Young's modulus $E = 190$ GPa, Poisson's ratio $\nu = 0.3$, tangent modulus $E_t = 6600$ MPa, yield strength $\sigma_y = 430$ MPa. The model is represented by FEM's discretization with 2009 nodes and 1440 hexahedron elements.

The total displacement of the corner point G (see Fig. 3(a)) is illustrated in Fig. 4, the obtained result is compared to ANSYS result and shows good agreement. In Fig. 4, we can observe that the displacement of point G increases linearly from the initial loading step to the 8th step. This is because the material deforms elastically. Then, in the subsequent steps (i.e., from 8th to 10th), the displacement of point G increases nonlinearly indicating the material has undergone plastic deformation. From the 10th loading step to the 20th step, the load gradually decreases to zero, while the displacement of point G starts to decrease linearly as the material exhibits elastic recovery properties.

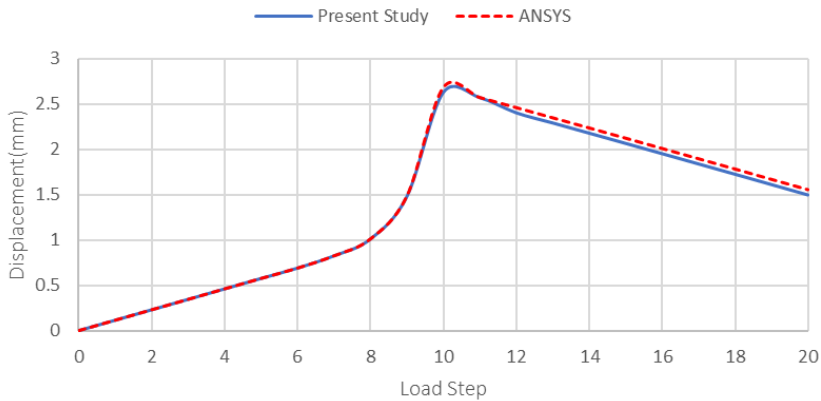


Fig. 4. The variation of displacement at the corner point G with respect to the computational step

When the model is unloaded after undergoing plastic deformation, it cannot back to its initial state because of the plastic strain. Fig. 5(a) shows the configuration of the initial state and unloading state, the difference between the two configurations comes from the plastic strain. Fig. 5(b) shows the configuration of the fully loaded state and unloading state, the difference between the two configurations comes from the nature of the material elasticity which is known as “springback”, it mentions the elastic recovery of material.

Fig. 6 demonstrates the springback behavior of metal under force. During torsion, the material surpasses its yield strength for permanent deformation. Upon unloading, the stress returns to zero along the elastic modulus slope. The permanent deformation is therefore less than what is designed into the part unless springback is taken into account.

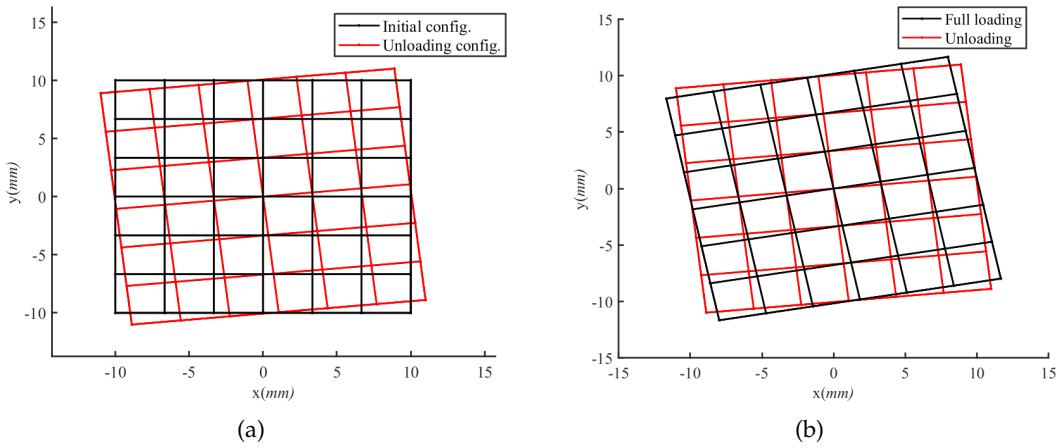


Fig. 5. (a) The initial and unloading configuration, (b) The full loading and unloading configuration

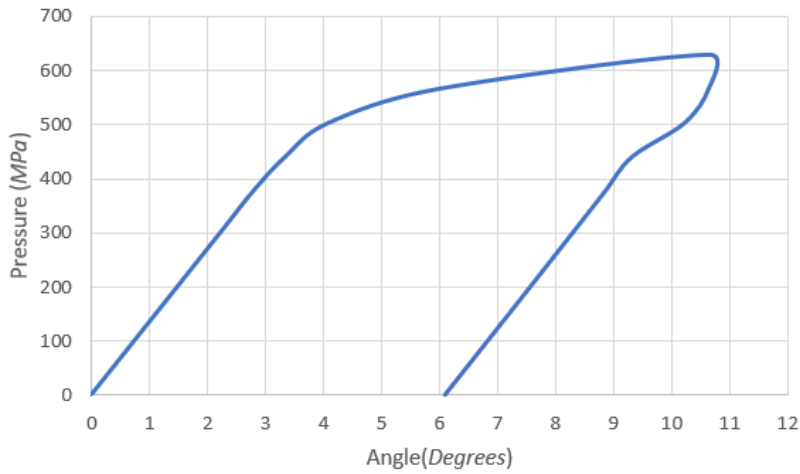


Fig. 6. Pressure-angle curve during the forming process

From Table 2, it is observed that when one wants to twist a square column an angle α , the required angle to twist is approximate 1.4282α . It shows that calculating the springback phenomenon in the metal forming process is very important.

Table 2. The springback value of angle α

	Angle (α)
Full loading	10.65°
Unloading	6.09°
Springback	4.56° (42.82%)

4. CONCLUSIONS

This study has achieved its objectives by exploring the nonlinearity material behavior. The method for solving nonlinear systems is based on the Newton–Raphson technique, and the plastic characteristics are computed through the return-mapping algorithm. The springback phenomenon in three-dimensional problems with material nonlinearity was discussed via numerical examples. The development of a Matlab program to analyze the springback phenomenon in a three-dimensional problem has been successfully accomplished, and the results have been compared and evaluated.

DECLARATION OF COMPETING INTEREST

The authors declare that they have no known competing financial interests or personal relationships that could have appeared to influence the work reported in this paper.

ACKNOWLEDGEMENT

We acknowledge Ho Chi Minh City University of Technology (HCMUT), VNU-HCM for supporting this study.

REFERENCES

- [1] X. A. Yang and F. Ruan. A die design method for springback compensation based on displacement adjustment. *International Journal of Mechanical Sciences*, **53**, (2011), pp. 399–406. <https://doi.org/10.1016/j.ijmecsci.2011.03.002>.
- [2] P.-A. Eggertsen and K. Mattiasson. On constitutive modeling for springback analysis. *International Journal of Mechanical Sciences*, **52**, (2010), pp. 804–818. <https://doi.org/10.1016/j.ijmecsci.2010.01.008>.
- [3] M. Rashid and C. Liebert. *Finite element analysis of a lifting portable offshore unit*. PhD thesis, Chalmers University of Technology Goteborg, Sweden, (2015).
- [4] W. L. Xu, C. H. Ma, C. H. Li, and W. J. Feng. Sensitive factors in springback simulation for sheet metal forming. *Journal of Materials Processing Technology*, **151**, (2004), pp. 217–222. <https://doi.org/10.1016/j.jmatprotec.2004.04.044>.
- [5] R. Wagoner and M. Li. Simulation of springback: Through-thickness integration. *International Journal of Plasticity*, **23**, (2007), pp. 345–360. <https://doi.org/10.1016/j.ijplas.2006.04.005>.
- [6] D. M. Krahmer, R. Polvorosa, L. N. López de Lacalle, U. Alonso-Pinillos, G. Abate, and F. Riu. Alternatives for specimen manufacturing in tensile testing of steel plates. *Experimental Techniques*, **40**, (2016), pp. 1555–1565. <https://doi.org/10.1007/s40799-016-0134-5>.
- [7] N.-H. Kim. *Introduction to nonlinear finite element analysis*. Springer US, (2015). <https://doi.org/10.1007/978-1-4419-1746-1>.
- [8] W. Lai, T. Yu, T. Q. Bui, Z. Wang, J. L. Curiel-Sosa, R. Das, and S. Hirose. 3-D elasto-plastic large deformations: IGA simulation by Bézier extraction of NURBS. *Advances in Engineering Software*, **108**, (2017), pp. 68–82. <https://doi.org/10.1016/j.advengsoft.2017.02.011>.